Influence of charge transfer doping on the morphologies of C_{60} islands on hydrogenated diamond C(100)- (2×1)

Markus Nimmrich,¹ Markus Kittelmann,¹ Philipp Rahe,¹ Wolfgang Harneit,¹ Andrew J. Mayne,² Gérald Dujardin,² and Angelika Kühnle^{1,*}

¹Institut für Physikalische Chemie, Fachbereich Chemie, Johannes Gutenberg-Universität Mainz, Jakob-Welder-Weg 11, D-55099 Mainz, Germany

²Institut des Sciences Moléculaire d'Orsay, Bâtiment 210, Université Paris-Sud, F-91405 Orsay Cedex, France (Received 19 October 2011; revised manuscript received 21 December 2011; published 13 January 2012)

The adsorption and island formation of C_{60} fullerenes on the hydrogenated C(100)- (2×1) :H diamond surface is studied using high-resolution noncontact atomic force microscopy in ultrahigh vacuum. At room temperature, C_{60} fullerene molecules assemble into monolayer islands, exhibiting a hexagonally close-packed internal structure. Dewetting is observed when raising the substrate temperature above approximately 505 K, resulting in two-layer high islands. In contrast to the monolayer islands, these double-layer islands form extended wetting layers. This peculiar behavior is explained by an increased molecule-substrate binding energy in the case of double-layer islands, which originates from charge transfer doping. Only upon further increasing the substrate temperature to approximately 615 K, the wetting layer desorbs, corresponding to a binding energy of the charge transfer-stabilized film of 1.7 eV.

DOI: 10.1103/PhysRevB.85.035420 PACS number(s): 68.37.Ps, 68.43.Hn, 68.43.Vx

I. INTRODUCTION

Hydrogenated diamond surfaces have received great attention in recent years due to the fact that they exhibit a p-type surface conductivity upon exposure to air. This finding is rather surprising since undoped diamond is an insulator with a band gap of 5.5 eV.2 The effect has soon been exploited to design novel field-effect transistors, but has only been understood years later when Maier et al. proposed the transfer doping model.⁴ According to this model, electrons from the diamond valence band can transfer into molecules adsorbed on the surface, leaving a hole behind within the surface layer (see model in Fig. 1). This is possible only because the hydrogenation of the diamond surface lifts the valence band maximum (VBM) from -5.9 eV to -4.2 eV. When molecules having an electron affinity in this energy range adsorb on the surface, transfer doping can occur. These kinds of adsorbates can, for example, be found dissolved in a surface water layer, explaining the emergence of surface conductivity upon exposure to air. The existence of a water wetting layer is, however, not a prerequisite for transfer doping. What is needed is simply a molecular species with very high electron affinity. C₆₀, exhibiting an electron affinity of 2.7 eV, has been identified as a promising candidate for well-controlled diamond transfer doping.^{5,6} Despite the gap of 1.5 eV to the VBM of hydrogenated diamond, it has been shown first theoretically⁷ and later experimentally,^{5,8} that C₆₀ can, indeed, induce surface conductivity in hydrogenated diamond even in the absence of water. Inspired by this finding, efforts have been made to study the adsorption of fullerenes on hydrogenated diamond surfaces in more detail.^{8,9} However, no study exists so far addressing the consequences of charge transfer doping on the C₆₀ island morphologies on hydrogenated diamond.

Here, we investigate the island formation of C_{60} upon adsorption on C(100)- (2×1) :H diamond surface using noncontact atomic force microscopy (NC-AFM) in ultrahigh vacuum

(UHV). Upon deposition at room temperature (RT), monolayer (ML) islands are formed having a typical size of several tens of nanometers in diameter. When annealing the substrate to approximately 505 K, the dewetting barrier appears to be overcome and C₆₀ molecules from the first layer hop into the second layer. In sharp contrast to the as-deposited structures, the resulting double-layer islands wet the surface, extending over many hundreds of nanometers in diameter. Complete desorption is achieved only when further increasing the substrate temperature to approximately 615 K. This peculiar evolution from a dewetting single-layer to a wetting double-layer film is explained by an increased molecule-substrate binding energy due to layer-dependent charge transfer doping. We present a simple electrostatic model, providing an explanation why single layer islands tend to dewet from the surface while double-layer films form a wetting layer.

II. METHODS

Experiments were performed at RT in a UHV system with a base pressure lower than 1×10^{-10} mbar. The system is equipped with a variable-temperature atomic force microscope (VT AFM 25 from Omicron, Taunusstein, Germany) and an amplitude controller and phase-locked loop detector (easyPLL Plus from Nanosurf, Liestal, Switzerland) for oscillation excitation and signal demodulation. In the frequency modulation mode, the main measuring signal is the shift of the resonance frequency. Depending on the feedback loop settings, either constant frequency shift images (topography channel) or constant height images (frequency shift channel) are obtained. The image type [topography (z), or frequency shift (Δf)] and scan directions are indicated in the displayed data. We use *n*-doped silicon cantilevers (NanoWorld, Neuchâtel, Switzerland) with resonance frequencies of about 300 kHz (type PPP-NCH), excited to oscillate with an amplitude of

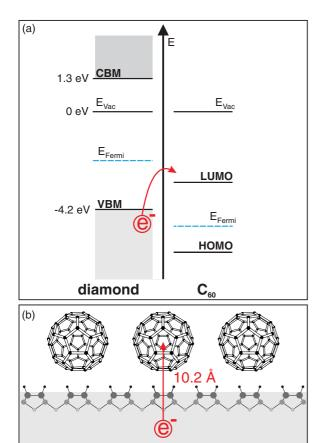


FIG. 1. (Color online) (a) Electronic levels of diamond (left) and C_{60} (right), illustrating the electron transfer from the diamond valence band maximum (VBM) to the lower unoccupied molecular orbital (LUMO) in C_{60} . (b) Spacial charge separation after electron transfer from diamond to C_{60} results in a distance of 10.2 Å as calculated in Ref. 10.

about 10 nm. Prior to their use, cantilevers were Ar⁺ sputtered at 2 keV for 5 min to remove contaminants.

The type IIa high-purity CVD diamond samples of $3.0 \times 3.0 \times 0.5 \,\mathrm{mm^3}$ in size used in this study were purchased from Diamond Detectors (Poole, UK). The samples are undoped. According to the supplier, the impurity concentration is below 1 ppm, with nitrogen being the largest portion. The investigated diamond surfaces were etched and hydrogenated *ex situ* in a hydrogen plasma prior to use, as described in detail elsewhere. The hydrogenated diamond samples were transferred into the UHV system and annealed to approximately 900 K in order to remove adsorbed contaminants from exposure to air. This procedure is known to provide reasonably clean C(100)- (2×1) :H surfaces. C(100)-C(

Prior to C_{60} deposition, the diamond samples were imaged with NC-AFM to analyze the structure on the atomic scale and the purity of the diamond surface. As observed before, ¹³ some protrusions cannot be removed by means of thermal desorption. Those surface features are likely to be nanodiamonds or adsorbates covalently bound to hydrogen-free surface areas. The C_{60} fullerenes (MER Corporation, Tuscon, Arizona; purity of 99.95%) were deposited onto the surface under UHV conditions by sublimation from a Knudsen cell held at a temperature of about 650 K. This cell temperature

corresponds to a flux of approximately 0.01 ML/s as measured with a quartz crystal microbalance (Inficon IC5 controller). During the deposition process, the substrate was kept at RT. The samples were transferred into the AFM situated in the same UHV system immediately after deposition. Any subsequent annealing of the samples was done in the same UHV system. The annealing temperature was measured using a thermocouple mounted at the sample stage about 2.5 cm away from the sample. The temperature specifications given in this work correspond to temperatures expected at the diamond sample based on an individual calibration curve supplied by the manufacturer (Omicron, Taunusstein, Germany).

III. EXPERIMENTAL RESULTS

A. As-deposited island structure

Upon deposition of approximately 0.07 ML C_{60} onto a sample held at RT, islands are formed having a typical size of several tens of nanometers in diameter. Figure 2(a) shows a representative NC-AFM image of the as-deposited situation at RT. The average area of these islands corresponds to approximately 700 nm². The formation of these islands demonstrates that the diffusion barrier is overcome at RT. As can be seen from the height profile shown in Fig. 2(b), the prevalent height of the islands is 0.9 nm \pm 0.1 nm, corresponding to single-layer C_{60} islands.

The molecular islands do not exhibit a clear hexagonal or trigonal shape as observed on other dielectric substrates. $^{14-16}$ Instead, a statistical analysis of island edges reveals two preferred directions. These two directions coincide with the [011] and $[0\overline{1}1]$ directions of the C(100)-(2 × 1):H surface. This finding demonstrates the structural influence of the underlying C(100)-(2 × 1):H substrate on the preferred orientations of the C₆₀ islands.

Repeated scanning over the single-layer islands readily results in the formation of double-layer structures, indicating that the single-layer islands represent a thermodynamically unstable configuration. A detailed view of such a double-layer island is shown in Fig. 3(a). The internal structure of the islands is hexagonal close-packed, as can be seen in Fig. 3(b). Due to the geometrical difference of the hexagonal C_{60} bulk structure

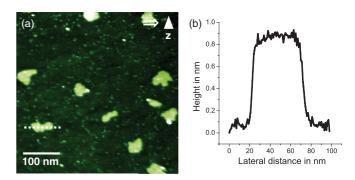


FIG. 2. (Color online) Topography NC-AFM image showing C_{60} fullerene islands on C(100)- (2×1) :H. (a) Overview of the as-deposited structure at RT after depositing 0.07 ML of C_{60} . (b) Height profile as indicated by the dashed line in (a), revealing a height of approximately 0.9 nm corresponding to a single layer of C_{60} .

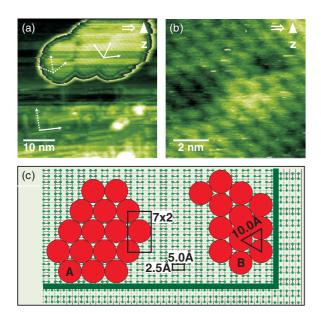
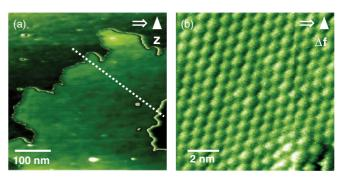


FIG. 3. (Color online) (a) Topography NC-AFM image showing the C_{60} orientation in relation to the C(100)-(2 × 1):H surface directions, which are pointed out by the dotted/solid pair of arrows in the lower left corner. The island consists of two domains rotated by 30°, as indicated by the dotted and the solid arrows. (b) Drift-corrected topography NC-AFM image showing individual C_{60} fullerenes aligning in a nearly hexagonal close-packed arrangement. (c) Model of the two domains.

with the rectangular surface structure, two island domains emerge, rotated by 30°. Occasionally, these two domains are apparent even within one single island, as shown in the island given in Fig. 3(a). Here, the structure of the underlying substrate is resolved together with the internal structure of the C₆₀ island. After correcting the image for thermal drift, we determined that the two domains are rotated by $30.4^{\circ} \pm 2.9^{\circ}$, in good agreement with the model shown in Fig. 3(c). This model is based on arranging a hexagonal lattice with lattice periodicity of 10.0 Å onto the rectangular lattice of the C(100)- (2×1) :H surface with dimensions of a = 2.52 Å and b = $5.04 \ \text{Å}$. A nearly hexagonal arrangement of the C_{60} molecules can be achieved by forming a $c(7 \times 2)$ superstructure (domain A). However, the terraces on the substrate are smaller than the typical island size. Thus, the C₆₀ islands extend on adjacent terraces, where the substrate directions are rotated by 90°. This results in a second domain (domain B) and readily explains the existence of two domains rotated by 30° as observed in the experiment. Interestingly, the geometrical match of the domain B with the underlying substrate is not as good as for domain A, indicating that the intermolecular interactions are decisive for the resulting molecular arrangement.

B. Island structure after annealing

A prominent change is observed upon annealing the C_{60} covered sample to a temperature of approximately 505 K. As can be seen in Fig. 4(a), the islands have grown in size, now extending over more than 12000 nm^2 in area. At the same time, the number of island is drastically decreased. As before, the observed internal structure is hexagonal [Fig. 4(b)]. Moreover, the islands exhibit a height of approximately 1.9 nm, as can be



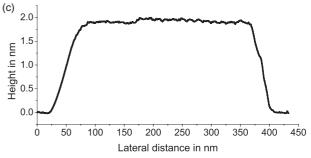


FIG. 4. (Color online) Topography NC-AFM images showing a C_{60} fullerene island on C(100)- (2×1) :H after annealing. (a) Island formed after annealing a sample covered with 0.07 ML C_{60} to approximately 505 K. (b) High-resolution image revealing the hexagonally packed inner structure. (c) Line profile as indicated in (a) revealing an island height of approximately 1.9 nm, corresponding to two layers of C_{60} .

seen from the height profile given in Fig. 4(c), corresponding to two layers of C_{60} . Thus, a clear transition is observed from small single-layer islands to an extended wetting film with a height of two layers.

C. Complete desorption

To further characterize the interaction between the molecular film and the underlying substrate, we determined the temperature above which complete desorption occurred. Complete desorption is achieved by annealing the substrate to a temperature in the range of 573 to 653 K. This finding corresponds well with previous high-resolution electron energy loss spectroscopy (HREELS) results, reporting multilayer desorption at temperatures of 473 K, while complete desorption has been achieved at 573 K. A rough estimate can be obtained for the desorption enthalpy using Redhead's formula for the desorption enthalpy.

$$E_{\text{des}} = T_{\text{des}} \cdot k_B \left\{ \ln \left(\frac{\nu \cdot T_{\text{des}}}{\beta} \right) - 3.64 \right\}$$
 (1)

where $E_{\rm des}$, $T_{\rm des}$, k_B , ν , and β are the desorption enthalpy, the corresponding desorption temperature, the Boltzmann constant, the attempt frequency, and the heating rate. A value of $E_{\rm des}=1.7~{\rm eV}\pm0.1~{\rm eV}$ is obtained for an average desorption temperature of 613 K, when using an attempt frequency of $\nu=10^{13}~{\rm s}^{-1}$ and a heating rate of $\beta=2~{\rm K/s}$. Interestingly, the desorption enthalpy is slightly larger than the sublimation enthalpy of crystalline C_{60} , around 1.65 eV, 18 which explains why multilayer desorption occurs at temperatures below

complete desorption. In other words, the binding energy of C_{60} to the hydrogenated diamond surface is larger than the binding of C_{60} molecules among each other in a solid crystal. This finding is in agreement with the fact that an extended wetting layer is found after moderate annealing. However, when considering the chemically inert nature of the hydrogenated diamond surface, the comparatively high interaction energy appears surprising.

IV. DISCUSSION

In order to explain the unexpected high binding energy of the double-layer films, we now discuss the influence of charge transfer doping on the binding energy of the double-layer film. As single-layer islands are found to dewet at approximately 505 K, a very rough estimate of the binding energy of single-layer C₆₀ molecules to the hydrogenated diamond surface can be given, being in the order of 1.4 eV. This value can be compared to the desorption temperature of C_{60} from the hydrogenated silicon surface, Si(100)-(2 \times 1):H. While this surface is chemically very similar to hydrogenated diamond, there is an important difference; there is an absence of charge transfer doping. Sanvitto et al. have measured a desorption temperature of C_{60} fullerenes from the Si(100)- (2×1) :H surface of approximately 503 K,19 corresponding to a desorption enthalpy of 1.3 eV. This desorption enthalpy agrees with van-der-Waals bound physisorbed C₆₀ molecules. However, this value is considerably smaller than that measured for the desorption enthalpy of the double-layer films on hydrogenated diamond, namely 1.7 eV. Thus, an additional effect in the order of 0.3 to 0.4 eV is expected to arise from the fact that charge transfer doping is possible on hydrogenated diamond. Transfer doping has been demonstrated to be considerably smaller for single-layer films than for higher coverages.⁵ This finding has been explained by the fact that electrostatic repulsion is more pronounced in single-layer films, hindering an efficient electron transfer. For double-layer films, in contrast, many-body effects reduce electron-electron repulsion and facilitate electron transfer. This is expressed in an effective increase in the electron affinity when comparing single-layer films with bulk C_{60} , as has been shown in Ref. 5. Thus, we expect a significant contribution of transfer doping for the double-layer films, but not for the single layer films, nicely explaining why the single-layer film dewets, while the double-layer film wets the surface. As a simple estimate for the contribution of charge transfer doping to the binding energy of the double layer to the substrate, we consider the electrostatic interaction arising from the spatial separation of electrons and holes. Based on calculations by Sque et al., 10 the spatial separation of electron and hole amounts to 10.2 Å upon adsorption of a C_{60} fullerene onto the $C(100)(2 \times 1)$:H surface. Taking this value literally, we can estimate the Coulomb attraction, amounting to 1.4 eV per transferred electron. To arrive at a meaningful estimate for the contribution of transfer doping to the binding energy, we need to consider the doping efficiency (surface hole density in diamond divided by C₆₀ coverage). The doping efficiency can be estimated to be as low as 10^{-2} to 10^{-3} . This estimate has, however, been calculated based solely on the measured surface conductance of the samples. Consequently, the obtained value is valid only when no immobile charge carriers exist that contribute to the doping process but not to the conductivity. As a large number of immobile charge carriers are likely to be present, the true doping efficiency might be considerably higher. Based on the very simple estimate made above, we obtain a doping efficiency in the order of 0.2 to 0.3. Given the simplicity of the picture drawn here for estimating the contribution of the charge transfer doping to the binding energy of a double-layer C₆₀ film, the agreement of the energy ranges is surprisingly good. However, we want to stress that we do not claim to give a definite quantitative but qualitative description of the contribution of charge transfer doping, which manifests itself in a peculiar transition from a dewetting to a wetting molecular layer.

V. CONCLUSIONS

C₆₀ fullerenes deposited onto the hydrogenated diamond C(100)- (2×1) :H surface reveal a peculiar transition from dewetting single-layer to wetting double-layer films. After deposition at RT, islands are observed with an average area of about 700 nm². Upon annealing the substrate to 505 K, the dewetting barrier is overcome, indicating a rather weak interaction of C₆₀ molecules from the single layer with the underlying substrate, which can be roughly estimated to 1.4 eV. In contrast to this finding, the resulting two-layer high islands form a wetting film, extending over more than 12000 nm² in area. These extended films indicate a rather strong interaction with the substrate, which is estimated to 1.7 eV. This considerable increase in interaction energy can be understood by considering the influence of charge transfer doping on the binding energy. Charge transfer doping is greatly reduced for single-layer films, but becomes significant in the case of double-layer films. A simple model considering electrostatic attraction accounts for approximately 1.4 eV of interaction energy in addition to simple van-der-Waals attraction. This model explains the unexpected high interaction energy in the case of double-layer films and provides an explanation for the transition from a dewetting single-layer to a wetting double-layer structure.

ACKNOWLEDGMENTS

This work has been supported by the Volkswagen-Stiftung through the program "Integration of molecular components in functional macroscopic systems".

^{*}kuehnle@uni-mainz.de

M. I. Landstrass and K. V. Ravi, Appl. Phys. Lett. 55, 975 (1989).
C. D. Clark, P. J. Dean, and P. V. Harris, Proc. R. Soc. A 277, 312 (1964).

³M. Itoh and H. Kawarada, Jpn. J. Appl. Phys. **34**, 4677 (1995).

⁴F. Maier, M. Riedel, B. Mantel, J. Ristein, and L. Ley, Phys. Rev. Lett. **85**, 3472 (2000).

- ⁵P. Strobel, M. Riedel, J. Ristein, and L. Ley, Nature (London) **430**, 439 (2004).
- ⁶P. Strobel, M. Riedel, J. Ristein, L. Ley, and O. Boltalina, Diam. Relat. Mater. **14**, 451 (2005).
- ⁷J. P. Goss, B. Hourahine, R. Jones, M. I. Heggie, and P. R. Briddon, J. Phys. Condens. Matter **13**, 8973 (2001).
- ⁸P. Strobel, J. Ristein, L. Ley, K. Seppelt, I. V. Goldt, and O. Boltalina, Diam. Relat. Mater. **15**, 720 (2006).
- ⁹T. Ouyang, K. P. Loh, D. Qi, A. T. S. Wee, and M. Nesladek, Chem. Phys. Chem. **9**, 1286 (2008).
- ¹⁰S. J. Sque, R. Jones, S. Oeberg, and P. R. Briddon, J. Mater. Sci.: Mater. Electron. **17**, 459 (2006).
- ¹¹E. Tranvouez, E. Boer-Duchemin, A. J. Mayne, T. Vanderbruggen, M. Scheele, R. Cartwright, G. Comtet, G. Dujardin, O. Schneegans, P. Chrétien *et al.*, J. Appl. Phys. **106**, 054301 (2009).

- ¹²K. Bobrov, A. Mayne, G. Comtet, G. Dujardin, L. Hellner, and A. Hoffman, Phys. Rev. B 68, 195416 (2003).
- ¹³M. Nimmrich, M. Kittelmann, P. Rahe, A. J. Mayne, G. Dujardin, A. v. Schmidsfeld, M. Reichling, W. Harneit, and A. Kühnle, Phys. Rev. B 81, 201403R (2010).
- ¹⁴S. A. Burke, J. M. Mativetsky, R. Hoffmann, and P. Grütter, Phys. Rev. Lett. **94**, 096102 (2005).
- ¹⁵S. A. Burke, J. M. Mativetsky, S. Fostner, and P. Grütter, Phys. Rev. B 76, 035419 (2007).
- ¹⁶M. Körner, F. Loske, M. Einax, A. Kühnle, M. Reichling, and P. Maass, Phys. Rev. Lett. **107**, 016101 (2011).
- ¹⁷P. A. Redhead, Vacuum **12**, 203 (1962).
- ¹⁸J. Abrefah, D. R. Olander, M. Balooch, and W. J. Siekhaus, Appl. Phys. Lett. **60**, 1313 (1992).
- ¹⁹D. Sanvitto, M. De Seta, and F. Evangelisti, Surf. Sci. **452**, 191 (2000).